# Evidence for Temperature-Dependent Conformational Changes in the L-Lactate Dehydrogenase from *Bacillus stearothermophilus*†

Michael Kotik and Herbert Zuber*

*Institut für Molekularbiologie und Biophysik, Eidgenössische Technische Hochschule-Hönggerberg, CH-8093 Zürich, Switzerland*

*Received February 7, 1992; Revised Manuscript Received June 1, 1992*

ABSTRACT: L-Lactate dehydrogenase from *Bacillus stearothermophilus* (BSLDH) has been shown to change its conformation in a temperature-dependent manner in the temperature range between 25 and 70 °C. To provide a more detailed understanding of this reversible structural reorganization of the tetrameric form of BSLDH, we have determined in the presence of 5 mM fructose 1,6-bisphosphate (FBP) the effect of temperature on far-UV and near-UV circular dichroism (CD), Nile red-binding to the enzyme surface, NADH binding, fluorescence polarization of fluorescamine-labeled protein, and hydrogen–deuterium exchange. In addition, we have analyzed the temperature dependence of the dimer–tetramer equilibrium of this protein by steady-state enzyme kinetics in the absence of FBP. The results obtained from these measurements at various temperatures can be summarized as follows. No changes in the secondary-structure distribution are detectable from far-UV CD measurements. On the other hand, near-UV CD data reveal that changes in the arrangements of aromatic side chains do occur. With increasing temperature, the asymmetry of the environment around aromatic residues decreases with a small change at 45 °C and a more pronounced change at 65 °C. Nile red-binding data suggest that the BSLDH surface hydrophobicity changes with temperature. It appears that decreasing the surface hydrophobicity may be a strategy to increase the protein stability of the active enzyme. We have noted significant alterations in the thermodynamic binding parameters of NADH above 45 °C, indicating a conformational change in the active site at 45 °C. The hydrodynamic volume of BSLDH is also temperature dependent. In the presence of 5 mM FBP, we interpret the data as an increase in hydrodynamic volume above 45 °C due to tertiary structure rearrangements in the stable tetrameric form. In the temperature range between 20 and 55 °C, we have observed in the absence of FBP a steady increase of the hydrodynamic volume, caused by the temperature dependence of the dimer⇌tetramer equilibrium. Above 55 °C a reversible oligomerization reaction has been detected probably involving denaturation events on the protein surface. FBP has a significant impact on the flexibility of the BSLDH structure as shown by hydrogen–deuterium exchange experiments. Further, this technique has been used to monitor the overall structural flexibility of the enzyme as a function of temperature.

Enzymes from thermophilic organisms differ from those of mesophilic organisms in stability and temperature dependence of activity. A comparison of the primary structures of thermophilic and mesophilic lactate dehydrogenases (LDH)[1] (Zuber, 1978, 1981a, 1988) or other enzymes (Argos et al., 1979; Zwickl et al., 1990) has revealed characteristic and temperature-related amino acid substitutions. High stability against thermal denaturation and enough flexibility to perform the crucial steps in catalysis are the two contrasting requirements that must be fulfilled by a thermophilic enzyme (Zuber, 1978, 1981b; Fontana, 1988; Jaenicke & Závodszky, 1990). Particularly thermophilic enzymes are often exposed to a wide temperature span in vivo. It is believed that the temperature-dependent reorganization of enzyme structures has its origin in the need for the enzyme to have at each temperature the optimal structure with respect to stability and flexibility (Zuber, 1981a; Wrba et al., 1990). Reversible temperature-dependent conformational changes have been described in a number of proteins from meso- and thermophilic organisms (Massey et al., 1966; Kayne & Suelter, 1968; Lehrer & Barker, 1970; Matsunaga & Nosoh, 1974; Zuber, 1981a; Chakerian et al., 1987). The basis for these studies has been the occurrence of discontinuities in Arrhenius plots, generally ascribed to multiple protein forms in equilibrium with each other. Although nonlinear Arrhenius plots may well indicate temperature-related conformational transitions, it is important to confirm this finding by other physical techniques. This is especially true when using overall enzymatic rate constants like $k_{cat}$, because in this case it is possible to obtain discontinuities in Arrhenius plots as different reaction steps become rate-limiting at different temperatures without the need of a conformational change. A conformational reorganization taking place at 45 °C in the L-lactate dehydrogenase from the thermophile *Bacillus stearothermophilus* (BSLDH) has been thought to be the cause for the strong temperature dependence of $k_{cat}$ and $K_m$ values (Stangl, 1987) and of the NADH binding to the enzyme (H.-P. Schär and H. Zuber, unpublished results; Zuber, 1981a). Recently, temperature-dependent conformational changes have been identified in the extremely thermostable D-glyceraldehyde-3-phosphate dehydrogenase from *Thermotoga maritima* (Wrba et al., 1990). It seems that the reorganization of the enzyme structure may be correlated to the functional adaptation of the conformation to different temperatures.

* Address correspondence to this author.

† This work was supported by the Eidgenössische Technische Hochschule Zürich, by Kredit Unterricht and Forschung, and by the Schweizerischer Nationalfonds, Grant 31-27711.89.

[1] Abbreviations: LDH, L-lactate dehydrogenase; BSLDH, LDH from *B. stearothermophilus*; CD, circular dichroism; FBP, fructose 1,6-bisphosphate; TEA, triethanolamine hydrochloride; NADH, reduced nicotinamide adenine dinucleotide.

0006-2960/92/0431-7787$03.00/0 

For several reasons, we have identified BSLDH as a suitable target enzyme for investigations of temperature-related conformational changes. It is a highly stable enzyme (Schär & Zuber, 1979), and its gene has been cloned and sequenced (Barstow et al., 1986; Zülli et al., 1987). It is the most thoroughly studied microbial LDH with respect to FBP activation, quaternary structural properties (Clarke et al., 1986a; Zülli et al., 1990), analysis of the catalytic mechanism (Clarke et al., 1986b, 1989), folding/unfolding pathways (Smith et al., 1991), and genetic engineering of catalytically important residues resulting in new enzyme substrate specificities (Wilks et al., 1988, 1990; Luyten et al., 1989). Furthermore, the LDH from *B. stearothermophilus* has been crystallized in two complexes, and the structures of these complexes have been solved (Piontek et al., 1990; Wigley et al., 1992). In addition, the important contribution of the $\alpha$–B helix for LDH stability has been recently shown by site-directed mutagenesis experiments (Zülli et al., 1991).

It should be stressed that BSLDH exists in two quaternary structures, namely, in a dimeric or a tetrameric form (Clarke et al., 1985). The stable tetramer can most easily be observed in the presence of 5 mM FBP. FBP acts as both an activator of the pyruvate reduction reaction and a molecule that strongly stabilizes the tetrameric state of the enzyme (Clarke et al., 1989). In the absence of FBP a dimer $\rightleftharpoons$ tetramer equilibrium is observed with this enzyme. We present in this paper results which demonstrate that BSLDH adapts to different temperatures by specific conformational changes.

## MATERIALS AND METHODS

*Enzyme Purification.* *Escherichia coli* K12, strain HB 101, containing the cloned BSLDH gene (Zülli et al., 1987) was used for the enzyme isolation. The purification was carried out twice as previously described by affinity chromatography on oxamate–Sepharose (Schär & Zuber, 1979), with the exception that a heat denaturation step prior to the ammonium sulfate precipitation was included. The purified protein was estimated to be >98% as judged by SDS–polyacrylamide gel electrophoresis. A second source of the enzyme was *B. stearothermophilus* cells (NCIB 8924), provided by Boehringer Mannheim GmbH, Biochemical Division, Tutzing. No differences between the enzymes from the two sources could be detected. The BSLDH was stored as a 65% ammonium sulfate precipitate.

*Buffers.* As buffers either 100 mM TEA, 100 mM Bis-Tris (for kinetic measurements), or 10 mM sodium phosphate was used. The pH of the buffers was adjusted to 6.3 at the desired temperature in the absence or presence of saturating concentrations of FBP (5 mM).

*Kinetic Analysis.* Steady-state measurements were performed on a Zeiss PMQ 4 spectrophotometer equipped with a constant-temperature cell holder. After preincubation of enzyme and NADH at the desired temperature, the reaction was initiated by addition of the appropriate pyruvate solution. The reaction was monitored by following the change in the absorbance at 340 nm caused by the depletion of NADH. Depending on reaction conditions, enzyme concentrations between 2 and 15 nM subunits were used. Experimental data were fitted either to the Michaelis–Menten equation including substrate inhibition (Cleland, 1983) or the Hill equation using the nonlinear regression program ENZFITTER (Leatherbarrow, 1987).

*Analysis of Dimer–Tetramer Equilibrium.* The steady-state kinetic analysis of the dimer $\rightleftharpoons$ tetramer enzyme system was carried out according to Kurganov (1967). Briefly, if association of enzyme subunits is coupled to a change in enzymatic activity, the association reaction can be analyzed from the relationship between specific enzymatic activity and the subunit concentration. In the simplest case of a dimer-tetramer reaction

$$2D \overset{K}{\rightleftharpoons} D_2$$

where the specific enzymatic activity of the free dimer is equal to zero, the following expression holds (Kurganov, 1967):

$$a = a_2 \frac{(\sqrt{1 + 8KC_0} - 1)^2}{8KC_0} \quad (1)$$

where $K = [D_2]/[D]^2$ is an apparent equilibrium constant, $C_0$ is the total molar concentration of the enzyme calculated as dimers, and $a_2$ is the specific activity of dimer incorporated in the tetramer. The parameters $K$ and $a_2$ were obtained by fitting the experimental data to eq 1 using nonlinear regression (Leatherbarrow, 1987).

*Circular Dichroism.* CD spectra were recorded on a JASCO J-710 spectropolarimeter. In the far-UV region (260–182 nm), 0.2-mm path length cells were used at a protein concentration of 250 $\mu$g mL$^{-1}$, whereas in the near-UV (330–250 nm), 1.0-cm path length cells were used at a protein concentration of 1 mg mL$^{-1}$. The absorbance at 280 nm was measured for each CD sample. The subunit concentration was calculated by using the extinction coefficient of $30.57 \times 10^3$ cm$^{-1}$ M$^{-1}$ (in the presence of 5 mM FBP) and $29.69 \times 10^3$ cm$^{-1}$ M$^{-1}$ (without FBP). Blanks of the solvent were subtracted from the measured spectra. The differential molar CD extinction coefficient, $\Delta\epsilon$, has the unit of L (mol residues)$^{-1}$ cm$^{-1}$ and is based on the molar concentration of the sum of residues in the BSLDH using an average residue weight of 109.98. The instrument was calibrated by using (+)-10-camphorsulfonic acid, assuming a $\Delta\epsilon$ of 2.36 cm$^{-1}$ M$^{-1}$ at 290.5 nm (Chen & Yang, 1977). Estimates of the secondary structure from the CD spectra were calculated using reference circular dichroism spectra of proteins that have a known secondary structure, in combination with singular value decomposition (SVD) and a variable selection procedure (Johnson, 1988). The following recommended selection criteria were maintained: (a) the sum of secondary structures is between 0.90 and 1.10; (b) the secondary structures are greater than –.05; and (c) the fit of the reconstructed CD lies within the noise level of experimental data, i.e., the root square of error is less than 0.22.

*Binding of Nile Red.* A strong enhancement of the dye fluorescence upon binding to hydrophobic surfaces makes Nile red a useful compound for detection of hydrophobic patches on a protein surface (Sackett & Wolff, 1987). The binding study with Nile red was conducted on a SPEX Fluorolog-2 Model F112XI, using an excitation wavelength of 550 nm and monitoring emission at the maximum at 654 nm. The Nile red stock solution was prepared according to Sackett and Wolff (1987). BSLDH (2.5 mM subunits) was placed in a cuvette and positioned in the thermostatic cuvette chamber. After 10 min of equilibration, a 4-$\mu$L aliquot of a Nile red stock solution was added to the cuvette to a final concentration of 1 mM. Spectra were recorded after equilibration for 2 min at the same temperature. Unbound dye adsorbs onto quartz and becomes nonfluorescent. This decay reaction in 100 mM TEA in the measured temperature range is slow however and, therefore, can be neglected. Spectra obtained with the same procedure as above but without enzyme served as a base line correction.

*Fluorescence Polarization Measurements.* The steady-state polarization $P$, defined by the relationship

$$P = (I_{vv} - GI_{vh})/(I_{vv} + GI_{vh}) \quad (2)$$

where $G = I_{hv}/I_{hh}$, was calculated by measuring the horizontal and vertical emission signals simultaneously with the T-format instrument configuration. The excitation was vertical ($I_{vv}$ and $I_{vh}$, respectively) and horizontal ($I_{hv}$ and $I_{hh}$, respectively) to the emission plane.

*Binding Studies with NADH.* Fluorescence polarization measurements were performed with a SPEX Fluorolog-2 Model F112XI photon-counting spectrofluorometer in the T-format configuration. The excitation wavelength was 340 nm and the emission wavelength 460 nm. The change of the polarization signal of the NADH molecule upon immobilization on the enzyme is a convenient method to follow its binding (Clarke et al., 1985). The affinity of NADH to the enzyme was determined by using a solution of about 2 $\mu$M coenzyme to which enzyme was added from a stock solution to a final concentration of 30 $\mu$M subunits. $P_{max}$, the polarization signal of NADH saturated with protein, was estimated from a plot of $1/P$ versus $1/[\text{enzyme}]$ according to Bagshaw and Harris (1987). With the knowledge of $P_o$, the polarization signal of NADH alone, the measured fluorescence polarization intensities were converted to the concentration of bound ligand and fitted to the Scatchard equation for a protein with one binding site:

$$B = \frac{A_T F}{K_d + F} \quad (3)$$

where $B$ represents the concentration of bound ligand, $A_T$ is the total concentration of enzyme subunits, $F$ is the concentration of free ligand, and $K_d$ is the dissociation constant.

*Labeling of Enzyme and Analysis of Fluorescence Polarization Data with Perrin Equation.* Subunits (350 $\mu$M) of BSLDH were labeled with fluorescamine (purchased from Sigma) according to Clarke et al. (1985). Fluorescamine attached to the enzyme was excited with polarized light of 395 nm, and the horizontal and vertical emission at 475 nm was measured. Depolarization of fluorescence for the protein–dye conjugate was analyzed by Perrin's equation. A plot of $1/P$ versus the temperature to solvent viscosity ratio ($T/\eta$) should result in a straight line. Deviations from a straight line are usually interpreted in terms of changes in the hydrodynamic volume of a protein or the uncoupling of the motion of the attached dye molecule from the motion of the protein due to creation of rotating units of smaller equivalent volume at high temperatures. The measurements were performed in dilute buffer solutions (10 mM sodium phosphate, pH 6.3, with and without 5 mM FBP), hence the viscosity of water was used in all calculations (Weast & Astle, 1981).

*Hydrogen–Deuterium Exchange.* The increase in transmission at 230 nm with time was used for the measurements of the replacement reaction of amide hydrogen by deuterium, essentially as described by Englander et al. (1979). $D_2O$ buffers were prepared by dissolving anhydrous sodium dihydrogen phosphate in $D_2O$ to give a molarity of 10 mM. The pD was adjusted to 6.3 with some drops of a 5 N NaOH solution according to the relationship

$$pD = pH^* + 0.4$$

where pH* is the pH meter reading. When amide protons exchange with deuterium, the absorbance band shifts to the blue, producing a small change in the absorbance region of 200– to 230 nm. As the background absorbance of interfering side chains is high, 230 nm was chosen for detection of the peptide amide proton exchange, where the signal to background ratio is better. To avoid artifacts during the measurements, several precautions were taken. First, all solutions were filtered through 0.22-$\mu$m Millipore filters. Second, the initiation of the reaction was performed with a mixing device very similar to the device described by Gregory et al. (1983). Simply, the mixing device consists of a Teflon cap, which fits onto a 1-cm cuvette, and a piston, through which the sample may be dispensed manually into $D_2O$. The mixing device allows the equilibration of the sample to the required temperature in a thermostated cuvette holder and the release of a 50-$\mu$L protein solution in $D_2O$ without perturbations in temperature caused by the mixing. Third, the duration of the measurements was restricted to 10 min because of a possible instrumental base line drift. The exchange reaction was started by pushing the mixing piston twice. The number of photons passing through the cuvette at 230 nm was registered with a sampling rate of 0.2 s/point. A deuterium lamp served as the light source, and the double monochromator and the cuvette holder were from Zeiss. The light which passed through the cuvette was collected by an EMI 9750QB photomultiplier. The power line voltage was electronically stabilized. All parts of the spectrophotometer were allowed to warm up for several hours before use. An EG&G Princeton Applied Research analog-digital converter was used as a storage unit. The data were subsequently smoothed by a moving average routine with a smooth width of 10 points. The measurements were performed in 10 mM sodium phosphate, pH 6.3, at an absorbance of 0.4 at 280 nm.

## RESULTS

*Association of Enzyme.* Steady-state enzyme kinetics in the absence of FBP revealed a relationship between the specific activity of BSLDH and the concentration of dimeric enzyme. The formation of tetramers when the enzyme concentration is raised is described by a dimer to tetramer association constant (eq 1, see Materials and Methods). $K$ as well as the specific activity of the dimer incorporated into the tetramer, $a_2$, depend on the initial pyruvate concentration (Figure 1A). Therefore $K$ is an apparent constant only and will be replaced by $K'$. Pyruvate as the substrate induces the formation of tetramers: 0.2 mM pyruvate in the reaction mixture leads to a $K'$ of $1.7 \times 10^7$ $M^{-1}$ at the above-described conditions, whereas 2.5 mM pyruvate changes the association constant to $13.2 \times 10^7$ $M^{-1}$. It is obvious that higher pyruvate concentrations increase the specific activity of the enzyme as seen in Figure 1A. The temperature dependence of the two parameters $K'$ and $a_2$ describing the association reaction shows a complex pattern (Figure 1B). With increasing temperature there is an increase of the specific activity of the dimer incorporated in the tetramer until its maximum at 45 °C. Interestingly, we noted that there was a second maximum of specific activity in the temperature range of 50–57 °C. The apparent association constant has its maximum at 30 °C and decreases sharply beyond this temperature to a value of approximately $1 \times 10^7$ $M^{-1}$. The pyruvate-dependent association of BSLDH dimers in the absence of FBP leads to a lag in the time course for NADH depletion (Figure 2A). In addition, non-Michaelis–Menten kinetics were observed with this enzyme (Figure 2B). Significant substrate inhibition for pyruvate was found above 3 mM pyruvate in the presence of saturating amounts of FBP. Without FBP, however, a small sigmoidal deviation from Michaelis–Menten kinetics was detected. This deviation could be intensified by increasing the enzyme concentration (data not shown).

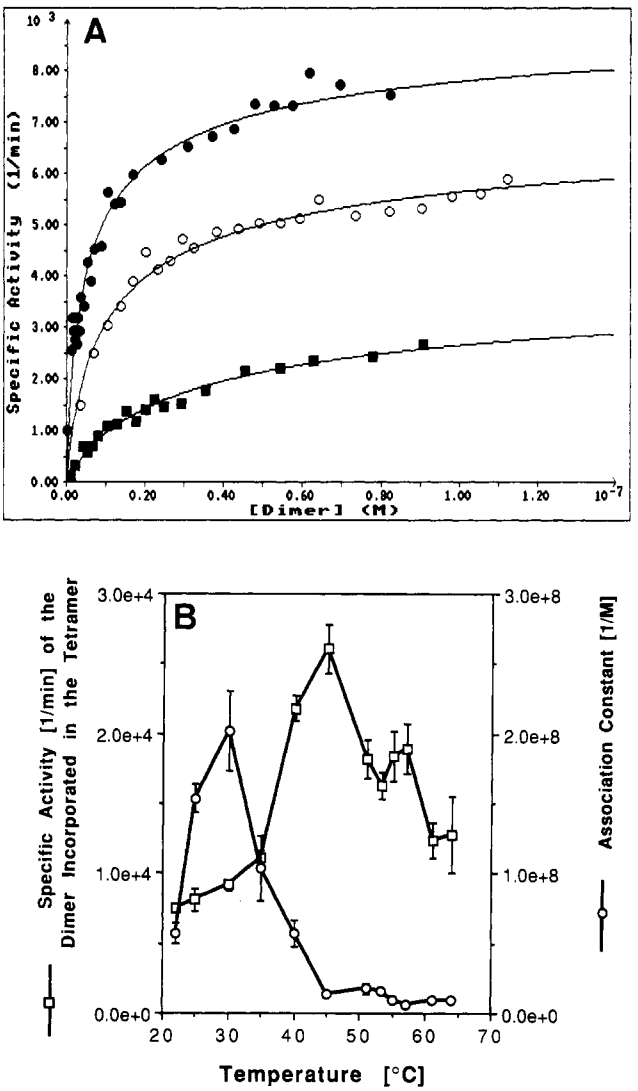


FIGURE 1: Relationship between enzyme concentration and degree of association of BSLDH. (A) The formation of tetramers as protein concentration is raised was determined by the relationship between specific enzymatic activity (expressed in M NADH $min^{-1}$ (M LDH dimers)$^{-1}$) and LDH concentration (expressed in dimers) using a nonlinear least squares fit to eq 1. Conditions of experiment: 25 °C, 100 mM Bis-Tris, pH 6.3, 200 μM NADH. Initial pyruvate concentrations: (■) 0.2, (○) 1.2, and (●) 2.5 mM. The apparent association constant $K'$ becomes larger with increasing initial pyruvate concentration, from $1.7 \times 10^7$ $M^{-1}$ (at 0.2 mM pyruvate) and $5.8 \times 10^7$ $M^{-1}$ (at 1.2 mM pyruvate) to $13.2 \times 10^7$ $M^{-1}$ (at 2.5 mM pyruvate). (B) Temperature dependence of the specific enzymatic activity of dimer incorporated in the tetramer ($a_2$) and of the association constant ($K'$). The two parameters were obtained by fitting the data points to eq 1. The experimental conditions were the same as above with the exception that the pyruvate concentration was held constant at 1.2 mM and the temperature was varied.

*Circular Dichroism.* The effects of temperature on the BSLDH conformation were analyzed by circular dichroism measurements in the near- and far-UV regions at a series of temperatures. In far-UV CD spectra the typical features of an α-helical protein, the presence of distinct bands at approximately 208 and 222 nm, appeared in the CD spectrum of BSLDH (data not shown). Spectra were collected in the presence and absence of FBP at various temperatures ranging from room temperature to 75 °C where the enzyme irreversibly denatured. No differences in the CD spectra from 20 to 55 °C could be detected. Above 55 °C the intensity of the CD signals slowly decreased with temperature, presumably due to the temperature-dependent hypochromicity of the peptide

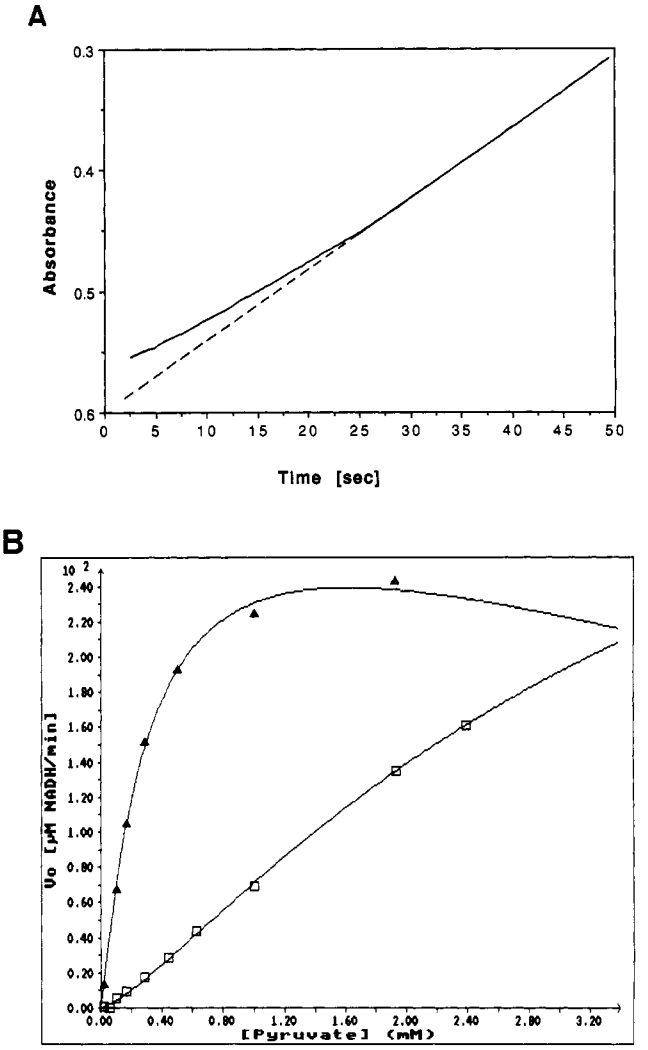


FIGURE 2: (A) Time dependence of NADH depletion catalyzed by *B. stearothermophilus* LDH in the absence of FBP at 25 °C. Assay was carried out as described under Materials and Methods. (B) Enzymatic activity of LDH from *B. stearothermophilus* at 50 °C versus pyruvate concentration. Oxidation of NADH was measured spectrophotometrically with 230 μM NADH and 11 nM LDH subunits. The measured rates (μM NADH/min) in the presence of 1.5 mM FBP (▲) and without FBP (□) were fitted to the Michaelis–Menten equation incorporating a term for substrate inhibition and to the Hill equation, respectively.

bond. Beyond 75 °C the CD curves drastically changed their shape and intensity due to enzyme denaturation. CD curves measured in the presence of 5 mM FBP and in its absence were analyzed up to 55 °C in order to obtain secondary structure information. The estimated distribution of secondary structures of BSLDH is as follows: 40% α-helix, 18% β-sheets, 13% turns, and 28% random coil. The sum of all secondary structures was close to 1.0, except for measurements above 55 °C, where the sum was in the range of 0.9–0.7. These latter estimates are therefore not as reliable as those conducted below 55 °C. The results of the CD secondary structure analysis are in good agreement with the secondary structure contents established by X-ray diffraction (Piontek et al., 1990). At 75 °C the enzyme began to denature, as indicated by the abrupt decrease of the α-helix contents and the simultaneous increase of the percent of random coil structures. Near-UV CD spectra obtained at different temperatures indicate an increase of structural flexibility in the asymmetric environment of aromatic residues with increase of temperature (Figure 3A). As a measure for the immo-

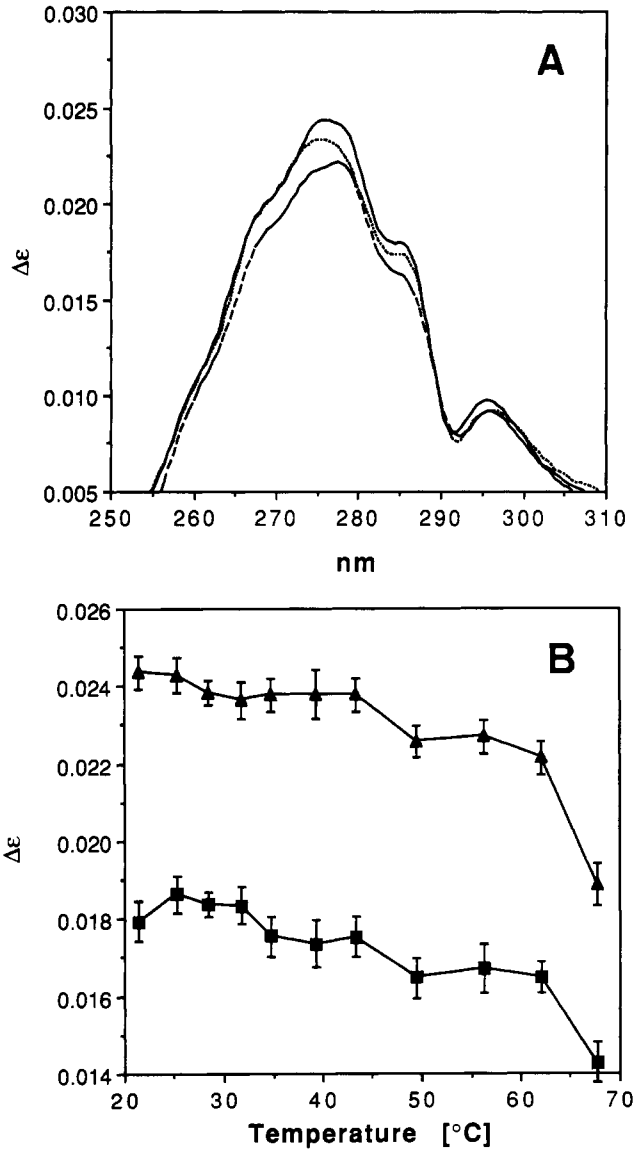


FIGURE 3: Near-UV circular dichroism of LDH from *B. stearothermophilus* in the presence of 5 mM FBP. (A) Spectra shown are base line subtracted scans in 10 mM sodium phosphate buffer, pH 6.3, at 21 (upper curve), 39 (middle curve), and 62 °C (lower curve). The accumulation of 10 spectra was performed by computer. Protein concentration, 34 μM subunits. (B) Temperature dependence of the peak magnitudes of the circular dichroic extinction coefficients of aromatic chromophores around 276 (▲) and 285 nm (■). Error bars indicate the estimated error from three identical measurements.

bilization of the aromatic residues and their environment, we used the peak heights at 276 and 285 nm. The temperature dependence of the circular dichroic extinction coefficients at the indicated wavelengths is shown in Figure 3B. With raising temperature, the asymmetry of the aromatic residues decreases with a small change occurring at approximately 45 °C. Above 62 °C, the aromatic residues are markedly less immobilized, although the protein does not denature below 75 °C.

*Effect of Temperature on Hydrodynamic Properties of Labeled BSLDH.* Fluorescamine-labeled enzyme was subjected to polarization measurements at a series of temperatures (Figure 4). Two different plots were obtained for the enzyme in the presence of 5 mM FBP and in the absence of FBP. As already mentioned, the BSLDH exists in its dimeric form at low enzyme concentrations, whereas saturating amounts of FBP change the quaternary structure of the enzyme to a tetramer (Clarke et al., 1985). This very well-characterized behavior of the enzyme is reflected in the Perrin plot as well, the polarization of the labeled enzyme with FBP present being higher (lower $1/P$ values in Figure 4) than without FBP. In the absence of FBP, the Perrin plot shows a concave behavior over the whole temperature range, indicating the formation of oligomers larger than dimers when temperature is raised. With FBP present, the Perrin plot shows a linear "low temperature" region until approximately 35 °C and a second linear "high temperature" region from 40 to 50 °C. Above 55 °C the polarization steeply increases with temperature, with a lag of some degrees to the polarization of the sample without FBP.

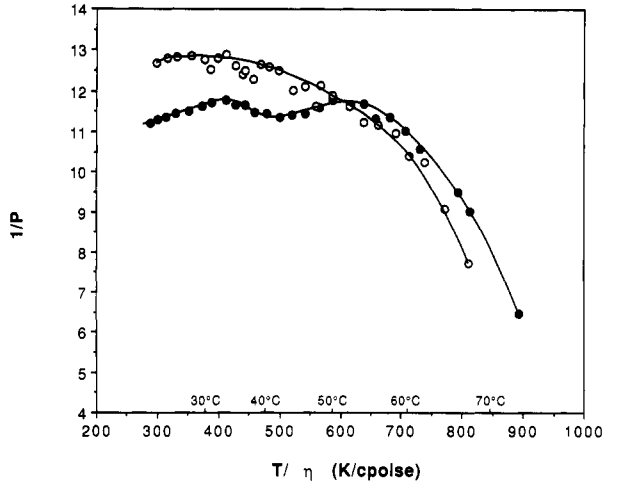


FIGURE 4: Perrin plot of fluorescamine-labeled LDH from *B. stearothermophilus*. The measurements were performed in 10 mM sodium phosphate buffer, pH 6.3, in the presence of 5 mM FBP (●) and in the absence of FBP (○) by varying the temperature.

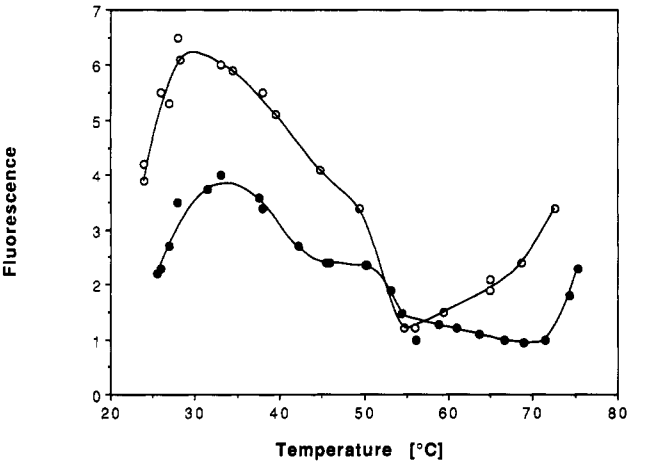


FIGURE 5: Temperature dependence of the amount of bound Nile red to the LDH from *B. stearothermophilus*. Measurements were performed in 10 mM sodium phosphate buffer, pH 6.3, with 2.5 μM LDH subunits and 1.0 μM initial concentration of Nile red. Fluorescence intensities of measurements without enzyme were subtracted. (○) Without FBP, (●) with 5 mM FBP.

*Detection of Surface Hydrophobicity.* Recently, Sackett and Wolff (1987) have shown that Nile red can be used as a tool to quantify the hydrophobicity on the surface of several proteins. The temperature-dependent binding of Nile red onto the surface of BSLDH is indicated in Figure 5. Several distinct ranges of surface hydrophobicity were detectable: an increase of hydrophobicity from 20 to 35 °C in the absence and presence of FBP and further, in the presence of 5 mM FBP a decrease to a minimum at 70 °C with an intermediary plateau region at 45–50 °C. Without FBP the surface hydrophobicity was almost doubled at low temperatures, and the minimum of hydrophobicity occurred at 55 °C with an increase again

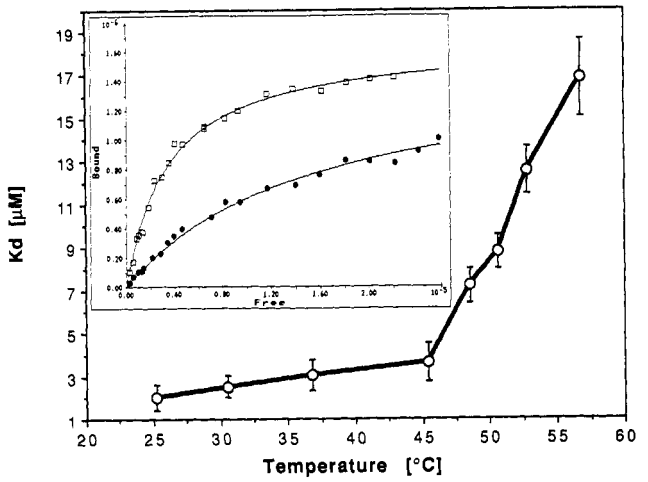


FIGURE 6: Temperature dependence of the NADH dissociation constant. The change of the fluorescence polarization of the coenzyme binding to the enzyme that was recorded as LDH was added to a cuvette containing 1.6 μM NADH in the absence of FBP. The data points were fitted according to a one-site binding model (Scatchard equation), and two examples at 45 °C ($K$ = 3.6 μM, □) and 56 °C ($K$ = 16.8 μM, ■) are shown in the inset.

Table I: Thermodynamic Parameters of NADH Binding on the LDH from *B. stearothermophilus*

| temp, °C | $\Delta G$, kJ mol$^{-1}$ | $\Delta H$, kJ mol$^{-1}$ | $\Delta S$, J mol$^{-1}$ K$^{-1}$ |
|---|---|---|---|
| 40 | −33.0 | −23 | +33 |
| 50 | −30.5 | −116 | −260 |

beyond this temperature. At 55 °C the amount of bound Nile red to the protein surface was identical in the presence of FBP and in its absence. In both cases, 5–10 °C before the enzyme started to denature, more Nile red molecules were bound to the enzyme surface, i.e., the surface hydrophobicity increased.

*Binding of NADH to BSLDH.* The titration of BSLDH with NADH at different temperatures revealed that the coenzyme binds noncooperatively to the protein (Figure 6), as has been previously shown by Clarke et al. (1985). The dissociation constant of NADH is remarkably dependent on temperature, the binding of the coenzyme being less tight above 45 °C. van't Hoff plots of the data were constructed to determine the equilibrium enthalpy change, $\Delta H$. The thermodynamic parameters of the binding and their temperature dependence are summarized in Table I. $\Delta H$ changes significantly between 40 and 50 °C by some 90 kJ mol$^{-1}$, with a concurrent change in sign of $\Delta S$. Thus, above the critical temperature of 45 °C more heat is liberated upon NADH binding under entropy reduction.

*Temperature-Dependent Changes in Flexibility of BSLDH Polypeptide Chain.* Hydrogen–deuterium exchange curves were obtained by following the time course of the decrease in the peptide–bond absorbance on deuteration at 230 nm. The experiments were performed with 5 mM FBP present and without FBP in order to investigate the effect of the activator on the conformational flexibility of the enzyme. The curves obtained at different temperatures are shown in Figure 7. The exchange of amide protons is characterized by a fast exchange reaction, presumably representing protons located near the protein surface, followed by a much slower exchange reaction (Figure 7A). Significant differences are seen between the temperature-dependent exchange reactions of amide protons in the presence of FBP and without FBP, when comparing Figure 7B with Figure 7C. 10 min after having started the exchange reaction, less counts were measured in the presence

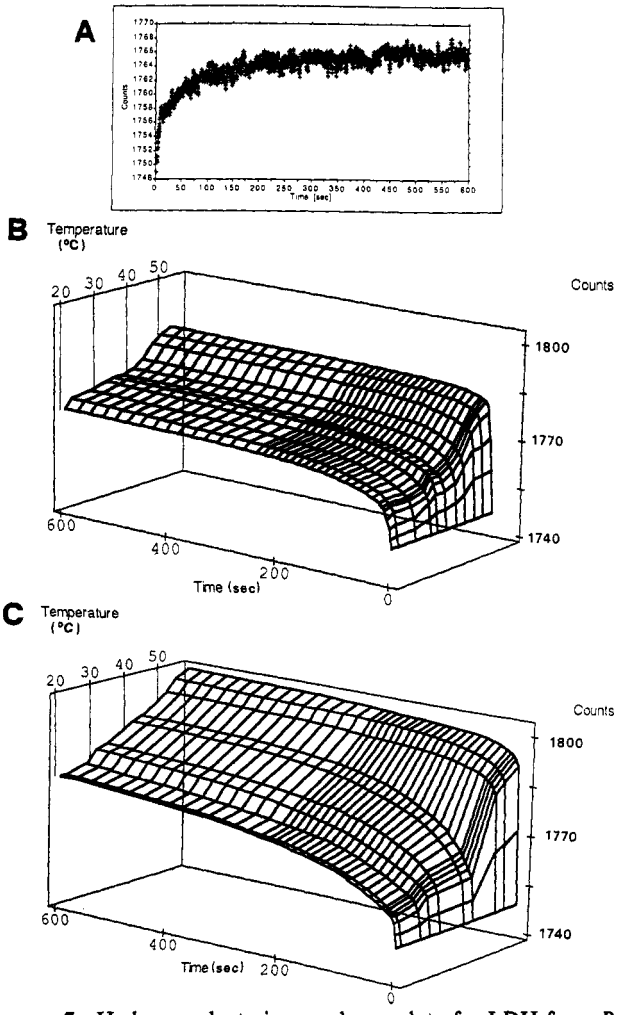


FIGURE 7: Hydrogen–deuterium exchange data for LDH from *B. stearothermophilus* in $D_2O$. (A) Example of a hydrogen–deuterium exchange curve obtained with an analog-digital converter after having smoothed the data by a running average smooth routine with a smooth width of 10 data points to reduce the noise. 50 μL of LDH in $H_2O$ was diluted into 1.0 mL of $D_2O$ buffer at pD 6.3, 37 °C, in the presence of 5 mM FBP. The number of counts at 230 nm was detected by using a sampling rate of 0.2 s/point. Hydrogen–deuterium exchange curves obtained at different temperatures were simplified by visual inspection and arranged in a 3D graph by plotting the amount of counts every 4.8 s, every 12 s from 24 s, and every 24 s from 240 s at various temperatures. Corresponding time points are connected. (B) Exchange curves in the presence of 5 mM FBP. (C) Exchange curves without FBP.

of FBP, i.e., the overall exchange reaction is slower. The stabilizing effect of FBP on the protein structure is mirrored in the reduced hydrogen–deuterium exchange reaction, especially pronounced above 45 °C. In both cases, namely, with and without FBP, the exchange curves become almost rectangular above 45 °C, indicating an accelerated exchange of the near-surface protons.

## DISCUSSION

Specific amino acid substitutions in LDHs (e.g., in the α–B helix), revealed by sequence comparison of meso- and thermophilic enzymes (Zuber, 1981a, 1988), and the statistical analysis of Menéndez-Arias and Argos (1989) point to decreased flexibility and increased hydrophobicity in α-helices of thermophilic enzymes as the main stabilizing principle. The question emerges of how these amino acid substitutions which are responsible for the improvement of the enzyme stability contribute to tertiary structure and dynamics. It is

now accepted that the difference in stability between meso- and thermophilic enzymes may be caused by subtle structural rearrangements (Jaenicke, 1991). Indications of minute structural reorientations within enzymes displaying different thermostabilities have been hinted at from the studies of Tidor and Karplus (1991). Below, we discuss to what extent the structure of BSLDH depends on temperature.

Secondary structure analyses of far-UV CD spectra with BSLDH obtained at different temperatures indicate that pronounced conformational rearrangements with shifts in the secondary structure distribution are absent. On the other hand, judging from CD spectra in the near-UV region (Figure 3), the environment of the immobilized aromatic residues is affected by temperature. At low temperature the packing of the aromatic side chains in their molecular environments is rigid whereas, with increasing temperature, the packing of the aromatic side chains becomes less tight. In particular, two transitions were seen in the fine structure of aromatic residues around 45 and 65 °C (Figure 3B).

The strong temperature dependence of the apparent association constant (from inactive dimer to active tetramer) in the absence of FBP (Figure 1B), as measured by steady-state enzyme activity at different enzyme concentrations, is probably caused by the combination of two effects. One is the increasing formation of tetramers with temperature (see Figure 4, without FBP); the other is the significant reduction of the enzyme affinity to pyruvate above 35 °C (Stangl, 1987). As pyruvate is able to shift the dimer–tetramer equilibrium toward the tetramer by preferentially binding to the tetramer, a reduced affinity to pyruvate leads automatically to a lower tetramer concentration and consequently to a lower dimer–tetramer association constant. The temperature dependence of the specific activity of the dimer incorporated in the tetramer revealed a complex pattern. The tetramer (without FBP) shows maximal activity at 45 °C. Above this temperature we observed a second peak of specific activity, indicating the presence of a conformational transition in the active site between 45 and 50 °C. The association–dissociation process of BSLDH in the absence of FBP leads to an enzymatic reaction with hysteretic behavior (Frieden, 1981), i.e., a lag in the time course for product formation (Figure 2A), because the inactive dimer $\rightleftharpoons$ active tetramer equilibrium is distorted slowly relative to the steady-state NADH depletion toward the active tetramer by the sudden presence of pyruvate. The sigmoidal dependence of the enzymatic reaction rate on the pyruvate concentration in the absence of FBP (Figure 2B) is an additional indication for a dimer $\rightleftharpoons$ tetramer reaction of BSLDH (Kurganov, 1968; Frieden, 1981). The magnitude of this deviation from Michaelis–Menten kinetics has been found to be directly proportional to the protein concentration (data not shown), as predicted by the theory (Kurganov, 1968; Frieden, 1981). In the presence of FBP, neither a dependence of specific activity on enzyme concentration nor sigmoidicity in a plot of enzymatic velocity versus pyruvate concentration could be detected in the temperature range of 20–55 °C, supporting the existence of only one stable form of BSLDH in the presence of saturating amounts of FBP.

The binding of NADH to the enzyme is strongly temperature dependent (Figure 6). Here, the transition at 45 °C from a low-temperature type of NADH binding, most probably corresponding to a low-temperature conformation of BSLDH, to a high-temperature NADH binding or BSLDH conformation is particularly evident. Above 45 °C more heat energy is liberated when NADH binds under entropy reduction (Table I). The question arises as to where this extra heat energy comes from. We can only speculate that the energetic state of the entire enzyme including the active site differs and that NADH is bound differently, above and below 45 °C. From the entropy reduction we can hypothetically assume that the binding of NADH above the transition temperature of 45 °C triggers a conformational change with a tighter packing of the enzyme.

A linear curve in a Perrin plot is usually interpreted as a strong indication for a rigid molecule without changes in the hydrodynamic volume when temperature or viscosity are varied. In the presence of FBP two separated linear sections are present in the Perrin plot of the fluorescamine-labeled enzyme (Figure 4). We interpret the anomaly that occurs in the temperature range of 35–40 °C as an overall change of the tetrameric protein conformation, whereby the hydrodynamic volume of the protein increases (less steep slope of the linear section between 40 and 50 °C in Figure 3), and the mobility of the fluorophore decreases (extrapolation to $T/\eta = 0$ giving a lower $1/P$ value). A second anomaly above approximately 53 °C is only interpretable as a result of oligomerization reactions, where oligomers of greater size than tetramers are being formed. Oligomers with a diameter up to about 600 Å (in contrast to native LDH with 90 Å) have been previously found by means of dynamic light scattering in the temperature range above 55 °C (H.-P. Schär and H. Zuber, unpublished results; Zuber, 1981b). It should be mentioned that the irreversible denaturation of the three-dimensional structure does not occur below approximately 75 °C. It is therefore likely that reversible denaturation processes on the protein surface are the reason for the observed oligomerization reaction. The denaturation of surface regions and the resulting oligomerization of BSLDH is probably responsible for the steep increase in the $K_m$ values for pyruvate and NADH beyond 58 °C (Stangl, 1987). In addition, it appears that the dimer–tetramer reaction of BSLDH is dependent on temperature, the tetramer being favored at higher temperatures (until 50 °C), as is seen from the Perrin plot curve obtained without FBP leaning against the curve obtained with FBP. In the absence of FBP, associates larger than tetramers are formed above 50 °C as in the case with FBP.

The surface hydrophobicity, as probed by the amount of bound Nile red, is also dependent on temperature (Figure 5). If the same technique is used with various mutant LDHs that denature at different temperatures ranging from 45 to 75 °C, a significant rise in the amount of bound dye is detected in each case prior to the actual denaturation taking place (M. Kotik, unpublished results). This obviously indicates that prior to denaturation hydrophobic patches on the protein surface are accessible to the dye. We conclude therefore that the binding of the hydrophobic dye to the protein surface is controlled mainly by the total hydrophobic areas present and only to a minor extent by the temperature itself. Hence it follows that the fluorescence of bound Nile red is a reliable and temperature-independent indicator of hydrophobic LDH surfaces. Further, it is likely that the dimer (measured without FBP) and the tetramer (measured with FBP) are very different in surface hydrophobicity at room temperature, as judged by the reduction of the number of accessible sites for the binding of the dye caused by tetramer formation. Since the dimer–tetramer equilibrium is shifted to the tetramer when temperature is raised (see discussion about the Perrin plot), the Nile red data in the absence of FBP are distorted by association–dissociation phenomena (i.e., the surface hydrophobicity decreases correspondingly to the formation of tetramers). However, the temperature-dependent alteration in

the amount of bound Nile red in the presence of FBP is caused by fluctuations of the surface hydrophobicity, resulting from conformational changes in the tertiary structure of the subunit. Worth mentioning is the increase of surface hydrophobicity between 30 and 40 °C (representing the low-temperature state) and the intermediary plateau region at 47 °C. The tendency to decrease the surface hydrophobicity with increasing temperature may be regarded as a strategy to delay the point of denaturation and to reach a certain functional state. Since hydrophobic interactions increase with temperature at least up to 60 °C (Némethy & Scheraga, 1962), it seems quite plausible that at higher temperatures the hydrophobic amino acids on the surface penetrate more strongly into the hydrophobic interior, lowering the concentration of hydrophobic interaction sites on the surface. Simultaneously, the hydrodynamic volume of the protein increases, probably caused by a counter-reaction where the hydrophilic residues are squeezed out. We suppose that conformational changes in the BSLDH structure are responsible for these measured effects in the temperature range of 20–50 °C. Above 55 °C, where reversible partial surface denaturation and the protein oligomerization occur, a noticeable diminution of the surface hydrophobicity was detected. Above 60 °C and without FBP, the surface hydrophobicity increased again, underlining the stabilizing effect of FBP in this temperature region (i.e., no increase of protein surface hydrophobicity until 70 °C in the presence of FBP).

The overall conformational flexibility of the enzyme, as revealed by hydrogen–deuterium exchange, is dependent on temperature as expected (Figure 7). These measurements give a good qualitative picture of the rigidity of the various temperature-dependent BSLDH conformers. FBP has a strong negative influence on the chain flexibility, particularly at temperatures above 45 °C. A comparison of the immobilization of aromatic residues (measured by near-UV CD) in the presence of FBP with that in the absence of FBP also points to a more flexible structure without FBP above 60 °C (data not shown). Numerous studies have shown that the accessibility of peptide hydrogens to solvent is influenced by ligand binding, suggesting that the ligands impose constraints on the dynamics of protein structures (De Weck et al., 1987, and references cited therein). It is therefore not astonishing that the point of thermal denaturation of BSLDH is increased by 3 to 5 °C in the presence of FBP (data not shown). Wrba et al. (1990) confirmed on the basis of D-glyceraldehyde-3-phosphate dehydrogenase from *T. maritima* that thermophilic enzymes have a reduced structural flexibility at room temperature when compared with mesophilic enzymes. The same results have been found by Varley and Pain (1991) when studying 3-phosphoglycerate kinases from yeast and *Thermus thermophilus*. By raising the temperature, the structure of the thermophilic enzyme becomes more flexible and the difference in activities between meso- and thermophilic enzymes that existed at low temperatures thereby vanishes. As far as one can judge from the hydrogen–deuterium exchange curves, the flexibility of the BSLDH structure above 45 °C is significantly higher (particularly at surface areas) than that at room temperature. This supports the proposition that both meso- and thermophilic enzymes have an equal chain flexibility and activity at their corresponding physiological temperatures (Zuber, 1981a; Jaenicke & Závodszky, 1990). In the context of this paper, it may be of interest that a further indication of a temperature-dependent conformational change has been found in the fact that BSLDH crystals grown at 50 °C crack upon cooling to room temperature (Stangl, 1987).

In summary, thermophilic BSLDH and, probably in general, thermophilic enzymes are ideal experimental systems for studying temperature-dependent conformational changes, since the available temperature span is larger than with mesophilic enzymes.

## ACKNOWLEDGMENT

We thank Dr. W. C. Johnson, Jr., for providing us with the software for protein secondary structure determination. We are grateful to F. Suter for his excellent computer assistance and to F. Luck for help with the hydrogen–deuterium exchange technique. Reading of the manuscript by Dr. J. Barber and K. Graham is gratefully acknowledged.

## REFERENCES

Argos, P., Rossmann, M. G., Grau, U. M., Zuber, H., Frank, G., & Tratschin, J. D. (1979) *Biochemistry 18*, 5698–5703.

Bagshaw, C. R., & Harris, D. A. (1987) in *Spectrophotometry & Spectrofluorimetry: A Practical Approach* (Harris, D. A., & Bashford, C. L., Eds.) pp 91–113, IRL Press, Oxford, England.

Barstow, D. A., Clarke, A. R., Chia, W. N., Wigley, D. B., Sharman, A. S., Holbrook, J. J., Atkinson, T., & Mington, N. T. (1986) *Gene 46*, 47–55.

Chakerian, A. E., Olson, J. S., & Matthews, K. S. (1987) *Biochemistry 26*, 7250–7255.

Chen, G. C., & Yang, J. T. (1977) *Anal. Lett. 10*, 1195–1207.

Clarke, A. R., Atkinson, T., Campbell, J. W., & Holbrook, J. J. (1985) *Biochim. Biophys. Acta 829*, 387–396.

Clarke, A. R., Evington, J. R. N., Dunn, C. R., Atkinson, T., & Holbrook, J. J. (1986a) *Biochim. Biophys. Acta 870*, 112–126.

Clarke, A. R., Wigley, D. B., Chia, W. N., Barstow, D., Atkinson, T., & Holbrook, J. J. (1986b) *Nature 324*, 699–702.

Clarke, A. R., Atkinson, T., & Holbrook, J. J. (1989) *Trends Biochem. Sci. 14*, 101–105.

Cleland, W. W. (1983) in *Contemporary Enzyme Kinetics and Mechanism* (Purich, D. L., Ed.) pp 253–265, Academic Press, New York.

De Weck, Z., Pande, J., & Kägi, J. H. R. (1987) *Biochemistry 26*, 4769–4776.

Englander, J. J., Calhoun, D. B., & Englander, S. W. (1979) *Anal. Biochem. 92*, 517–524.

Fontana, A. (1988) *Biophys. Chem. 29*, 181–193.

Frieden, C. (1981) in *Protein–Protein Interactions* (Frieden, C., & Nichol, L., Eds.) pp 289–314, John Wiley & Sons, New York.

Gregory, R. B., Crabo, L., Percy, A. J., & Rosenberg, A. (1983) *Biochemistry 22*, 910–917.

Jaenicke, R. (1991) *Eur. J. Biochem. 202*, 715–728.

Jaenicke, R., & Závodszky, P. (1990) *FEBS Lett. 268*, 344–349.

Johnson, W. C. (1988) *Annu. Rev. Biophys. Biophys. Chem. 17*, 145–166.

Kayne, F. J., & Suelter, C. H. (1968) *Biochemistry 7*, 1678–1684.

Kurganov, B. I. (1967) *Mol. Biol. 1*, 14–22.

Kurganov, B. I. (1968) *Mol. Biol. 2*, 351–363.

Leatherbarrow, R. J. (1987) ENZFITTER, Elsevier Biosoft.

Lehrer, G. M., & Barker, R. (1970) *Biochemistry 9*, 1533–1540.

Luyten, M. A., Gold, M., Friesen, J. D., & Jones, J. B. (1989) *Biochemistry 28*, 6605–6610.

Massey, V., Curti, B., & Ganther, H. (1966) *J. Biol. Chem. 241*, 2347–2357.

Matsunaga, A., & Nosoh, Y. (1974) *Biochim. Biophys. Acta 365*, 208–211.

Menéndez-Arias, L., & Argos, P. (1989) *J. Mol. Biol. 206*, 397–406.

Némethy, G., & Scheraga, H. A. (1962) *J. Phys. Chem. 66*, 1773–1789.

Piontek, K., Chakrabarti, P., Schär, H.-P., Rossmann, M. G., & Zuber, H. (1990) *Proteins: Struct., Funct., Genet. 7*, 74–92.
Sackett, D. L., & Wolff, J. (1987) *Anal. Biochem. 167*, 228–234.
Schär, H.-P., & Zuber, H. (1979) *Hoppe Seylers Z. Physiol. Chem. 360*, 795–807.
Smith, C. J., Clarke, A. R., Chia, W. N., Irons, L. I., Atkinson, T., & Holbrook, J. J. (1991) *Biochemistry 30*, 1028–1036.
Stangl, D. (1987) Ph.D. Thesis, Eidgenössische Technische Hochschule, Zürich.
Varley, P. G., & Pain, R. H. (1991) *J. Mol. Biol. 220*, 531–538.
Weast, R. C., & Astle, M. J., Eds. (1981) *Handbook of Chemistry and Physics, 62nd ed.* p F-42, CRC Press, Boca Raton, FL.
Wigley, D. B., Gamblin, S. J., Turkenburg, J. P., Dodson, E. J., Piontek, K., Muirhead, H., & Holbrook, J. J. (1992) *J. Mol. Biol. 223*, 317–335.
Wilks, H. M., Hart, K. W., Feeney, R., Dunn, C. R., Muirhead, H., Chia, W. N., Barstow, D. A., Atkinson, T., Clarke, A. R., & Holbrook, J. J. (1988) *Science 242*, 1541–1544.
Wilks, H. M., Halsall, D. J., Atkinson, T., Chia, W. N., Clarke, A. R., & Holbrook, J. J. (1990) *Biochemistry 29*, 8587–8591.
Wrba, A., Schweiger, A., Schultes, V., Jaenicke, R., & Závodszky, P. (1990) *Biochemistry 29*, 7584–7592.
Zuber, H. (1978) in *Biochemistry of Thermophily* (Friedman, S. M., Ed.) pp 267–285, Academic Press, New York.
Zuber, H. (1981a) in *32nd Colloquium der Gesellschaft für Biologische Chemie (Structural and Functional Aspects of Enzyme Catalysis)* (Eggerer, H., & Huber, R., Eds.) pp 114–127, Springer-Verlag, Berlin, Heidelberg.
Zuber, H. (1981b) in *Trends in the Biology of Fermentations for Fuels and Chemicals* (Hollaender, A., Rabson, R., Rogers, P., San Pietro, A., Valentine, R., & Wolfe, R., Eds.) pp 499–512, Plenum Press, New York.
Zuber, H. (1988) *Biophys. Chem. 29*, 171–179.
Zülli, F., Weber, H., & Zuber, H. (1987) *Biol. Chem. Hoppe-Seyler 368*, 1167–1177.
Zülli, F., Weber, H., & Zuber, H. (1990) *Biol. Chem. Hoppe-Seyler 371*, 655–662.
Zülli, F., Schneiter, R., Urfer, R., & Zuber, H. (1991) *Biol. Chem. Hoppe-Seyler 372*, 363–372.
Zwickl, P., Fabry, S., Bogedain, C., Haas, A., & Hensel, R. (1990) *J. Bacteriol. 172*, 4329–4338.